[7] T. P. Chow and A. J. Steckl, "Size effects in $MoSi_2$-gate MOSFET's," *Appl. Phys. Lett.*, vol. 36, pp. 297-299, Feb. 1980.
[8] S. P. Murarka, "Refractory silicides for integrated circuits," *J. Vac. Sci. Technol.*, vol. 17, pp. 775-792, Jul./Aug. 1980.
[9] T. N. Jackson and N. A. Masnari, "A novel submicron fabrication technique," *1979 IEDM Tech. Dig.*, pp. 58-61, Dec. 1979.
[10] W. R. Hunter, T. C. Holloway, P. K. Chatterjee, and A. F. Tasch, Jr., "New edge-defined vertical-etch approaches for submicrometer MOSFET fabrication," in *1980 IEDM Tech. Dig.*, pp. 764-767, Dec. 1980.
[11] —, "A new edge-defined approach for submicrometer MOSFET fabrication," *IEEE Electron Device Lett.*, vol. EDL-2, pp. 4-6, Jan. 1981.
[12] E. C. Jelks, G. L. Kerber, and H. A. Wilcox, "A simple method for fabricating lines of 0.15-μ width using optical lithography," *Appl. Phys. Lett.*, vol. 34, pp. 28-30, Jan. 1979.
[13] D. C. Flanders, "Replication of 175-Å lines and spaces in polymethylmethacrylate using X-ray lithography," *Appl. Phys. Lett.*, vol. 36, pp. 93-96, Jan. 1980.
[14] A. C. Ipri, "Sub-micron polysilicon gate CMOS/SOS technology," in *1978 IEDM Tech. Dig.*, pp. 46-49, Dec. 1978.
[15] D. E. Prober, M. D. Feuer, and N. Giordano, "Fabrication of 300-Å metal lines with substrate-step techniques," *Appl. Phys. Lett.*, vol. 37, pp. 94-96, July 1980.
[16] W. G. Oldham, A. R. Neureuther, C. Sung, J. L. Reynolds, and S. N. Nandgaonkar, "A general simulator for VLSI lithography and etching processes: Part II—application to deposition and etching," *IEEE Trans. Electron Devices*, vol. ED-27, pp. 1455-1459, Aug. 1980.
[17] T. P. Chow and A. J. Steckl, "Planar plasma etching of Mo and $MoSi_2$ using NF_3," in *1980 IEDM Tech. Dig.*, pp. 149-151, Dec. 1980.

High Resolution Fabrication of Josephson Microbridges

DANIEL E. PROBER, MEMBER, IEEE

Abstract—**Recent advances in fabrication techniques and performance of 100-nm-scale superconducting Josephson microbridges are reviewed. Fabrication requirements imposed by the desired electrical performance are discussed; these lead to very small device dimensions and a three-dimensional structure to ensure good cooling of the active region. Fabrication approaches based on electron-beam lithography and on edge-defined patterning with substrate steps both achieve the desired dimensions and geometries. The self-aligning step-edge approach is simpler and more versatile for dimensions <100 nm, however, and is also ideally suited for production of microbridges employing high-T_c refractory superconductors. Device performance for recent ultrasmall microbridge devices is summarized and assessed in terms of future limits.**

I. Introduction

JOSEPHSON junction electronics has demonstrated great promise for digital and analog circuit applications [1]-[3]. Fast digital circuits, low-noise microwave mixers, and ultrasensitive magnetometers have all been produced recently, and fundamental limits due to quantum mechanics can be foreseen. In the case of the mixers and magnetometers, these quantum limits have recently been reached [2]. Josephson devices have thus made fundamental advances in performance in many classes of electromagnetic devices.

Manuscript received April 1, 1981; revised June 22, 1981. This work was supported in part by the National Science Foundation.

The author is with the Section of Applied Physics, Yale University, New Haven, CT 06520.

In addition to achieving improved device performance, Josephson devices have also provided significant microlithographic challenges. The device structures are relatively simple, and unlike semiconductor devices, are not limited in minimum size by lengths such as depletion layer widths. Device performance typically improves as the size is reduced, even down to a size scale of a few nanometers (for point-contact devices [1]). As a result, Josephson devices represent an ideal proving ground for new device fabrication concepts. A variety of useful submicrometer fabrication approaches have resulted from studies on Josephson devices, and these techniques are now finding application in other areas of microelectronics and in submicrometer physics studies [4].

In this review we will discuss fabrication approaches which have been developed recently for producing Josephson microbridges in the size range $\lesssim 0.1$ μm. Microbridge devices use a thin metallic constriction to provide the Josephson-effect coupling between two large superconductors. A schematic of a microbridge is shown in Fig. 1. The microbridge is the thin-film analog of the metallic point contact, but with the thin-film advantages of ruggedness, reliability, and reproducibility. Though the properties of early devices were not notably reproducible, devices can now be made reproducibly with the advanced techniques we shall describe.

In addition to the construction devices—microbridges and point contacts, the other major class of Josephson devices is the tunnel junction, which uses a material barrier to obtain

0018-9383/81/1100-1368$00.75

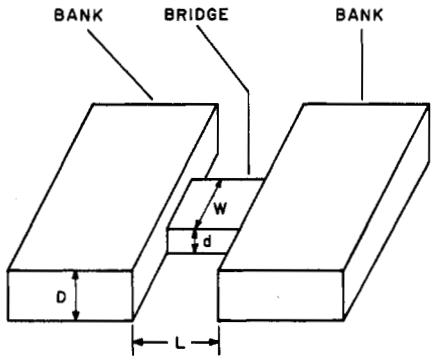

Fig. 1. Schematic of a variable-thickness microbridge device. The *bridge* in the center has dimensions of L, W, and d (length, width, and thickness). The *banks* are the two large superconducting electrodes, whose superconductivity is coupled through the bridge. The bank thickness is D. For $D \gg d$ and small bridge dimensions, the microbridge approaches the point contact structure.

weak coupling between two superconductors. Josephson digital circuits have been based exclusively on oxide-barrier tunnel junctions [3], and more recently, tunnel junctions have been employed in microwave mixers and in magnetometers. Due to their extremely small capacitance, microbridges and point contacts still have significant advantages for very-high-frequency operation, at frequencies $\sim 10^{12}$ Hz, and they may also allow a wider choice of material or operating temperature [5]. Recent reviews [3], [5]-[9] of Josephson device fabrication techniques have concentrated primarily on fabrication of tunnel junctions or micrometer-scale devices. However, as we shall discuss, only microbridges of size ≤ 0.1 μm appear to have the characteristics needed in the significant areas of application. We shall therefore focus in this review on issues of microbridge fabrication in the size regime $\lesssim 0.1$ μm.

II. Dimensional and Fabrication Requirements

Microbridge Josephson devices are based on the nonlinear response of the supercurrent flowing through a narrow filament linking two larger superconductors (see Fig. 1) [10]. The microbridge shown in Fig. 1 has *banks*, the two large superconductors, which are thicker than the *bridge*. This structure, known as the variable-thickness microbridge (VTB) configuration, has numerous advantages [10]-[12] over the uniform thickness configuration ($D = d$). Of primary importance is that the thick banks provide much more effective cooling of the power dissipated in the bridge $\sim V^2/R$. (A finite voltage occurs in the operating state.) The effects of Joule heating pose the primary limit on microbridge performance and applicability at high frequencies, and also at operating temperatures well below the transition temperature T_c. The variable-thickness configuration is thus essential, at least for microbridge structures made of a single material. The variable-thickness structure approaches the three-dimensional geometry of the point contact, which achieves excellent cooling, and analyses are the same for $D \gg d$ and L, W, and d sufficiently small.

The fundamental size scale for microbridges is set by the superconducting coherence length $\xi(T)$, the Ginzburg-Landau coherence length. For bridge length $L < \xi(T)$, the superconducting behavior approaches that of an ideal Josephson junction [10]; this is known as the depairing regime, and is the desired range of operation. Near T_c, the coherence length depends on temperature T as

$$\xi(T) = \xi(0)\left(\frac{T_c}{T_c - T}\right)^{1/2} \tag{1}$$

with $\xi(0)$ the coherence length at $T = 0$. $\xi(0)$ is a constant of the material, and for high resistivity materials depends on the electron mean-free path l as

$$\xi(0) \propto l^{1/2}. \tag{2}$$

Typical values of $\xi(0)$ range between 10 and 200 nm. Since microbridge operation over a wide temperature range is desirable, it is a length $\sim\xi(0)$ which sets the lithographic requirement on bridge size. For a variable-thickness geometry with $D \gg L$, a value of $L \sim \xi(0)$ should be satisfactory for both good Josephson properties [10] and reduced heating effects [12].

The material chosen for the bridge thus determines the required device dimensions. Good performance requires $L \sim \xi(0)$. However, superconductors with a high normal-state ($T > T_c$) resistivity are often desired. This is because in most microbridge applications, the microbridge impedance in the operating state is of the order of R, the bridge resistance above T_c. (Capacitive shunting is negligible for microbridges, but can be significant for tunnel junctions [8], [12].) For high-frequency detectors and mixers [13] a resistance of 10-100 Ω is desired to match impedances at the signal and IF frequencies. For magnetometers [14], a resistance of 1-10 Ω appears to be optimum for matching and noise considerations. For a microbridge with $D \gg d$, R is given by

$$R = \frac{\rho_n L}{Wd} \tag{3}$$

with ρ_n the normal-state film resistivity $\propto l^{-1}$. Therefore, ρ_n must be fairly large to achieve a high microbridge resistance. According to (2), the bridge size must then be quite small to keep $L \sim \xi(0)$. For example, for many metals a value of $\xi(0) \sim$ 20 nm is found for $\rho_n = 10^{-5}$ $\Omega \cdot$ cm. Thus there is a conflict between achieving high resistance and good Josephson performance, and the requirements on microbridge resistance lead to a rather stringent lithographic requirement: that all microbridge dimensions be less than about 0.1 μm. While series arrays of low-resistance microbridges are possible [9], with dimensional requirements somewhat relaxed, arrays have not yet led to improvements in the overall performance of microwave receivers.

Superconductors with a high transition temperature [5], based on transition-metal compounds and alloys, would be desired in most applications. These materials are also extremely rugged and stable, in contrast to the *soft* superconductors (e.g., Pb alloys) in common use today [3]. All high-temperature ($T_c > 10$ K) superconductors [5] have short coherence lengths, <10 nm. Even pure Nb, with $T_c = 9.2$ K, has a short coherence length, $\xi(0) = 40$ nm. The use of these *hard* superconductors for the bridge region will thus set very stringent dimensional constraints on microbridge size because of the very short coherence lengths.

An approach which has proven to be very effective in fabri-

cating high-T_c microbridges is to use the high-T_c superconductor only for the banks, and to use a different material for the bridge [10]. The bridge can be another superconductor with a different (usually lower) value of T_c; this is known as a S-S'-S microbridge. An alternate approach is to use a normal (nonsuperconducting) metal or semimetal; this is designated a S-N-S microbridge. The S-N-S structure has the advantage that the decay length ξ_n for the superconducting pairs coupling through the nonsuperconducting metal can be much larger than the coherence length of the high-T_c superconducting banks. Thus dimensional requirements on the bridge length are less stringent than when one uses the high-T_c superconductor for the bridge.

Another approach for utilizing high-T_c superconductors is to employ a granular superconductor in the bridge region [15], [16]. While the mechanisms which lead to Josephson-effect coupling in granular microbridges are not well understood, excellent device performance can still be obtained [16].

The ultimate practical goal of much of the research on microbridge devices would be the production of a microbridge with electrical characteristics equal to those of the best point-contact devices [11], [12], which have resistances of 10–150 Ω. Lesser performance would be quite satisfactory in most applications, however. The neck diameter inferred for point contacts is <10 nm [12], with the performance improving as the size is reduced. This defines the scale of the lithographic challenge for microbridge fabrication for single-material structures. Multiple-material structures (e.g., S-N-S) allow one to optimize bridge and bank properties somewhat independently, and also allow relaxed dimensional constraints. More complex fabrication procedures may be required in this case, however.

III. Fabrication Approaches and Performance Criteria

The earliest microbridges studied were of uniform thickness ($D = d$). These were made by mechanical scratching with a sharp diamond point, with photolithography techniques, or with electron-beam lithography [6], [9]. While the Josephson effect was clearly evident just below T_c, hysteresis effects due to thermal runaway occurred at lower temperatures. This hysteresis was due to the power dissipated, $\sim V^2/R$, which heated the bridge above T_c, so that superconductive (Josephson) coupling through the bridge was lost. A solution to these problems is to utilize the three-dimensional cooling of the variable-thickness microbridge configuration [11], [12]. (Very little heat is conducted away by the substrate in the immediate vicinity of the bridge, due to acoustic impedance mismatch.) A measure of the success of the heat removal is the width of the temperature interval below T_c for which the I-V curves are free of heating-induced hysteresis. This interval is defined as $\Delta T_{\text{no hyst}}$; a normalized quantity of

$$\Delta t_{\text{no hyst}} = \Delta T_{\text{no hyst}}/T_c \tag{4}$$

will be considered below for several variable-thickness microbridges. Ideally, $\Delta t_{\text{no hyst}} = 1$. A second quantity, the maximum voltage at which the ac Josephson effect can be observed, $V_{\max}$, provides a related measure of the effectiveness of the heat removal [11], [12].

There are basically two lithographic approaches for producing variable-thickness microbridges. The first approach uses direct lithographic patterning—either photolithography or electron-beam lithography. The minimum size is determined by the resolution of the lithographic process. Multiple-film depositions are employed, and typically two lithographic patternings are used [9], though resist masks for self-aligned multiple depositions are possible.

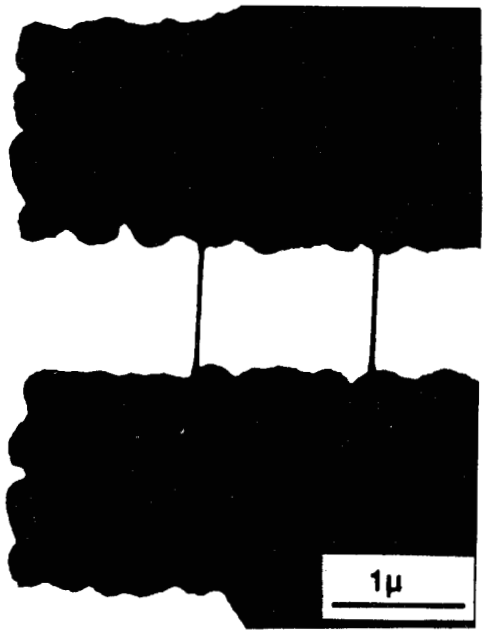

Fig. 2. Scanning-transmission electron micrograph of a pair of variable-thickness niobium microbridges produced with contamination-resist electron-beam lithography [19]. Contamination resist masks the thin Nb bridge film during Ar-ion etching. Thick Nb banks are produced with standard electon-beam lithography with a polymer resist. (Micrograph courtesy of Laibowitz and Broers.)

In the second major approach, steps etched in the substrate are used to define bridge dimensions. For dimensions <0.1 μm, this latter approach is both simpler and more versatile, as we shall discuss below.

IV. Direct Lithography

In the direct lithography approach with multiple patternings, the bridge is part of a longer strip of width W, over which the banks are deposited. With standard electron-beam lithography, S-N-S microbridges of $L = W = 200$ nm and $D/d = 2.5$ have been produced [17]. This resolution is similar to the limiting resolution obtainable with advanced optical lithography techniques [18]. While finer scale electron lithography is now possible on solid substrates [8], the smallest microbridges produced by direct lithography have been made with contamination-resist electron-beam lithography on thin-window substrates [19]. The contamination resist is used as a protective etch mask for Ar-ion etching. Niobium microbridges as small as $L = 20$ nm, $W = 70$ nm, with $D/d = 3$ were produced. Thin windows are employed to minimize electron backscattering from the substrate. A micrograph of a pair of microbridges produced with this contamination-resist technique is shown in Fig. 2.

With the direct lithography approach, films with different properties can be used for the bridge and for the banks. Use

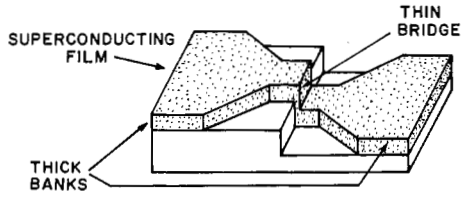

Fig. 3. Schematic of a variable-thickness microbridge formed over a substrate step edge. The step height determines the bridge length as $L = H - D$. Deposition direction is near the substrate normal. Bridge width is here defined by direct lithography—e.g., photolithography. (From [22].)

of a bridge film with moderately large electrical resistivity will allow a large value of R, while good bridge cooling can be obtained by using a high-thermal-conductivity (low-resistivity) film for the banks. S-N-S microbridges are thus an example of such a structure, where electrical and thermal properties can be optimized separately. However, as with any multiple-film approach, interdiffusion must be minimal. In addition, it is essential to remove any oxide layer and contamination due to resist processing immediately before deposition of the second film [9], [19]. This would usually be accomplished with Ar-ion etching. Ion etching can damage high-T_c superconductors [20]. Thus to form high-T_c S-N-S microbridges, the two films are deposited without breaking vacuum, and subtractive etching is employed to pattern the banks and bridge. Since high-T_c superconductors must be deposited onto a hot substrate [5], $T \sim 700°C$, interdiffusion during deposition, between films (if the normal metal is deposited first) or with the substrate, can also pose problems in fabricating high-T_c microbridges.

V. Step-Edge Lithography

The second major approach to microbridge fabrication, first used by Feuer and Prober [21], [22] is to use a step (or steps) in the substrate to define bridge length (and possibly other dimensions). A single film deposition can be used to form both the bridge and banks. A first version of this approach is illustrated in Fig. 3. Here, the step is ion-etched into the substrate and the metal film is deposited from an angle near normal, so that $d \ll D$. The key feature of this process is that the step height H determines bridge length as

$$L = H - D. \tag{5}$$

Because both D and H can be measured and controlled to an accuracy of <10 nm with standard thin-film techniques, L can be extremely small. Bridge lengths of $L = 40$ nm are easily achieved. In addition, the requirements of making D large and L small are not in direct conflict, as they are for direct patterning. Thus one can produce with the step-edge approach bridges with $D \gg L$, even for $L < 0.1$ μm. A further benefit is that interface and resist contamination problems are absent with this approach.

The bridge width in the example of Fig. 3 is defined by a direct lithographic process. Liftoff photolithography [18] was used by Feuer [22]. In general then, W will be significantly greater than L, and the bridge resistance will be low. In addition, the heat flow into the banks is not three-dimensional near the bridge. As a result, the electrical performance of these devices is not outstanding [22]. Still, such step-edge microbridges do serve to demonstrate the lithographic concept.

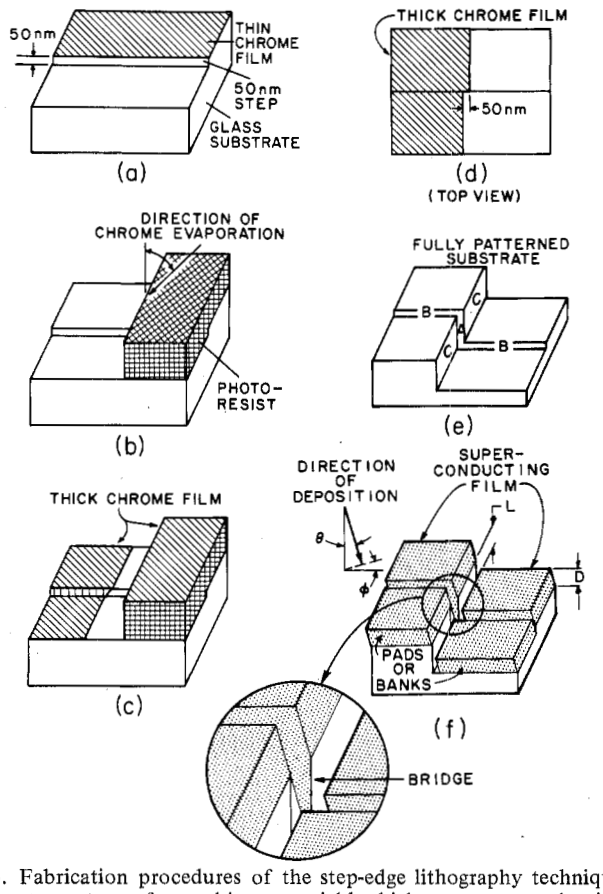

Fig. 4. Fabrication procedures of the step-edge lithography technique using two steps, for making a variable-thickness superconducting microbridge with a width $W \approx 50$ nm. Details of the process are given in the text. Chrome film is single hatched, photoresist is cross hatched, and superconducting metal film (Fig. 4(f)) is dark. Dimensions are not to scale. The diagram is drawn for the small ϕ limit, so the bridge thickness $d \ll D$ is not shown.

A method for producing a step-edge microbridge with $W \leqslant L$ is possible [21], and is depicted in Fig. 4. Here, two substrate steps are used, one to define the bridge length, the other to define the width. Starting with the fully patterned substrate, Fig. 4(e), the metal film is deposited at the angle shown, to coat the bridge region (region A) lightly, and the bank regions (regions B) heavily. The bridge length is again given by $L \approx H - D$, as in Fig. 3. For small θ and ϕ, the bridge width W is equal to the width of the jog (region A), which in this example is equal to the height of the initial substrate step, Fig. 4(a). Finally, the bridge thickness is given by $d = D \tan\theta \sin\phi$. Thus *all* bridge dimensions are determined by step and film heights and the deposition angle.[1]

The key element in producing the fully patterned substrate of Fig. 4(e) is producing thick chrome film with the sharp *jog*

[1] In our discussion we assume that the metal atoms stick at the exact point of impact. This idealized model is a standard assumption for most shadowing processes. Deviations from this model and resulting fabrication limits are discussed in [21] and [22]. To minimize agglomeration of the superconducting film, film deposition was at 77 K. Actual microbridge dimensions deviate only 10 to 20 nm from those of the idealized model, and these deviations are reproducible for each individual material.

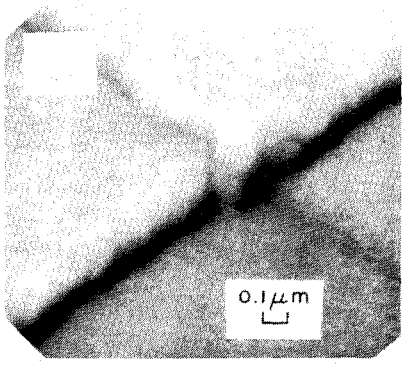

Fig. 5. SEM of a microbridge fabricated with the procedures of Fig. 4. A 0.1-μm size scale is shown. Perspective is like that for Fig. 4(f). The light regions in Fig. 5 are the superconducting metal film, and the dark regions are the edges of the substrate step which are not coated [regions C in Fig. 4(e)]. Dimensions of the bridge are $d = L =$ 60 nm, $W_{min} = 50$ nm, and $D = 240$ nm. The step height is 300 nm. (Dimensions cannot be determined directly from the micrograph due to foreshortening at this observation angle.)

along its edge, as shown in Fig. 4(d). This sharp jog is then transferred into the substrate with reactive ion-beam etching, and the chrome film is then chemically etched off. To form the jog, the thick chrome film is deposited at an evaporation angle of 45° from the substrate normal (Fig. 4(b)). This forms a "shadow" of the top edge of the photoresist pattern, which is smooth where it crosses the step (as shown) due to the spin-on application of the photoresist. However, the substrate has a small step already etched into it (Fig. 4(a)). Therefore, the shadow cast by the photoresist edge lies *farther away* where the photoresist is thicker (over the bottom of the step). After the photoresist is washed off in acetone, the chrome pattern in Fig. 4(d) remains. The height of the initial step, Fig. 4(a), has effectively been folded over onto the substrate by this shadowing procedure. Thus it is possible with optical lithography and this shadowing technique to produce three-dimensional microbridge structures which are substantially smaller than the optical diffraction limit [18]. This demonstrates the significant advantage of such a self-aligning fabrication approach.

A microbridge produced with the fabrication sequence of Fig. 4 is shown in Fig. 5. The bridge dimensions are $L = 50$ nm, $W_{min} = 50$ nm, $d = 60$ nm, and $D = 240$ nm. Though smaller microbridges have been produced with this technique [22], it is difficult to obtain high-contrast electron micrographs of these smaller structures. This is because the microbridge is on a solid substrate, so that transmission-electron microscopy, as was used for the micrograph of Fig. 2, is not possible. The micrograph in Fig. 5 was taken with a field-emission source high-resolution scanning electron microscope (SEM).

Table I lists the dimensions of the smallest variable-thickness microbridges fabricated with the double-step technique [21] and with electron-beam direct lithography using contamination [19] or conventional resists [17]. The edge-defined microbridges are seen to be somewhat smaller. Recently fabricated step-edge microbridges, including the In bridge in Table I, used Ni-Cr etch masks instead of Cr, because of the smaller grain size of Ni-Cr [22]. Also, oxygen reactive-ion-beam etching of a substrate coated with a 1-μm-thick layer of polyimide was

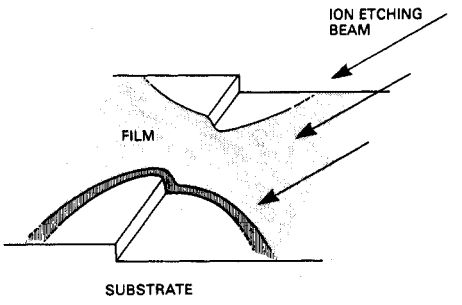

Fig. 6. Technique used to make NbN microbridge with a granular superconductor bridge region, defined by the step height. The bridge region is selectively thinned by ion etching. Step height is 75 nm. (From [16].)

TABLE I
MICROBRIDGE DIMENSIONS ACHIEVED WITH VARIOUS HIGH RESOLUTION PATTERNING TECHNIQUES[a]

Microbridge	Reference	Patterning Technique	Dimensions (nm) L	W	D
Pb-Cu-Pb	[17]	e-beam, polymer resist	200	200	150
Nb	[19]	e-beam, contamination resist	120	70	80
$Pb_{0.9}In_{0.1}$	[21]	step-edge	40	50	110
In	[21]	step-edge	200	<40	350

[a]Width at narrowest point is given. Values of bridge thickness d are all less than L.

used. The ratio of etch rates of polyimide and Ni-Cr is >25:1 [22], allowing very high aspect-ratio patterning.

Another successful utilization of the step-edge approach is by Claassen [16], as shown in Fig. 6. In this work, thin NbN films ($T_c \approx 12$ K), were sputtered onto a substrate with a 75-nm step, as in Fig. 3. The bridge width was patterned by photolithography. The bridge region was then thinned by Ar-ion-beam etching. (The bridge is preferentially exposed to the ion beam by the step.) After thinning, the bridge film was ~5 nm thick and partly discontinuous, behaving like a granular superconductor. The mechanisms leading to Josephson effect in granular superconductor bridges are not yet known [16]. Claassen's studies demonstrate, however, that for such granular materials one can have $L \gg \xi(T)$ and $W \gg \xi(T)$ and still achieve very good device performance (see below). The Nb microbridges formed by contamination lithography [19] also show some granularity effects [23], and also have $L \gg \xi(T)$. A variety of other high-T_c and refractory superconductors show Josephson effects when damaged or thinned in a region ≤ 1 μm in length [24].

A final example of the use of the step-edge concept is its utilization with a multimaterial structure, a S-N-S microbridge [25] of Nb_3Sn-Cu-Nb_3Sn. Nb_3Sn has a high T_c of 18 K, and would be widely employed in Josephson electronics, except that this material must be deposited at a substrate temperature >700°C. As shown in Fig. 7, the Nb_3Sn film was deposited from a direction so that it was discontinuous at the step. The substrate was heated during deposition of the Nb_3Sn, and, without breaking vacuum, the substrate was cooled and the

TABLE II
MICROBRIDGE PERFORMANCE DATA FOR SMALL VARIABLE-THICKNESS MICROBRIDGES AND FOR A HIGH-QUALITY POINT CONTACT[a]

	$R(\Omega)$	V_{max}(mV)	I_cR(mV)	$\Delta t_{no\ hyst}$	Mechanism of Josephson Effect	Reference
In	5	1.9	0.9	>0.6	Depairing ($L < \xi$)	[21]
$Pb_{0.9}In_{0.1}$	8	1.5	1.2	0.2	Depairing	[21]
Sn	0.3	3.7	1.3	>0.6	Depairing	[12]
Nb	20	0.4	0.3	0.4	Granular + Depairing	[19], [23]
NbN	30	1.5	0.5	0.5	Granular	[16]
Pb-Cu-Pb	0.3	2	0.06	0.5	S-N-S	[17]
Nb_3Sn-Cu-Nb_3Sn	1	4	1	0.8	S-N-S	[25]
Pb alloy-doped Si-Pb alloy	3	–	0.8	0.3	S-Semicond-S	[28]
Nb point contact	100	12.5	2	>0.6	Depairing	[29]

[a] $\Delta t_{no\ hyst}$ is the normalized temperature interval below T_c for which the I-V curves are free of heating-induced hysteresis; ideally, $\Delta t_{no\ hyst} = 1$. V_{max} is the maximum voltage at which the ac Josephson effect can be observed (see text). The product of the critical or maximum supercurrent I_c and the device resistance sets a second voltage limit on device operation (see [12]). The I_cR product listed here is taken for the lowest temperature at which the I-V curves are nonhysteretic. The depairing regime applies for short microbridges, $L < \xi$ (see text).

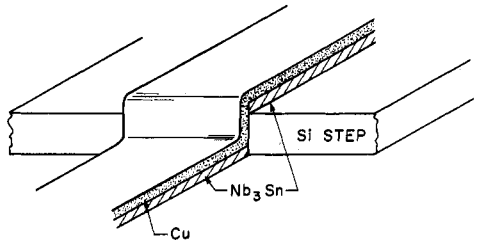

Fig. 7. S-N-S microbridge formed from high-T_c superconductor banks of Nb_3Sn and a Cu bridge. Depositions of the Cu and the Nb_3Sn films are from two different angles, to produce the structure shown. Bridge width is defined by photolithography. Step height is 120 nm. Sapphire substrate is not shown. (From [25].)

Cu film was deposited. The Cu film was deposited to coat the step fully, and thus was continuous over the step. The step height was ~120 nm. The performance of the first microbridges fabricated with this approach demonstrates the outstanding potential of the high-T_c films. For $L \sim 0.1$ μm and $W = 3$ μm, a device resistance of 1 Ω and nonhysteretic operation between 3 and 16.5 K are obtained. Higher device resistances should be possible. This fabrication approach of de Lozanne utilizes very effectively the dimensional and directional capabilities of the step-edge approach, and allows significant material flexibility. Indeed, the potential of the step-edge technique for meeting specific processing requirements is far from exhausted. The recent report [26] of a Nb-Bi-Nb microbridge using film-edge techniques serves to reinforce this point. Recent advances in high-contrast ion-etching techniques [27] should increase the range of applicability of the step-edge approach.

In Table II we compare performance data for a number of variable-thickness microbridges fabricated with the high-resolution techniques described in this review. We have also included the best microbridge produced by scratching with a diamond knife. Except for the low resistance of this bridge, its performance is otherwise excellent. (For this microbridge, ρ_n was low, $\sim 10^{-6}$ $\Omega \cdot$ cm.) Data are also included for a semiconductor-coupled device [28], analogous to the S-N-S structure but with a doped semiconductor instead of the normal metal bridge, and for the best point-contact device reported in the literature [29].

Among the high-resistance microbridge devices in Table II, no one structure or device has achieved the performance of the *ideal* point contact. Only a few applications, such as far-infrared mixers, require this ideal performance. Still, planar dimensions of 25 nm are now achievable with various advanced direct lithographic techniques [4], and, in combination with step-edge techniques, it should soon be possible to produce microbridges with performance like that of ideal point contacts.[2] With the use of high-T_c superconductors, the performance of future ultrasmall microbridges may even exceed that achieved to date with ideal Nb point contacts.

VI. CONCLUSIONS

The three-dimensional nature of the variable-thickness Josephson microbridge, Fig. 1, has stimulated productive developments in three-dimensional step-edge lithography approaches and in very-high-resolution direct lithography. The advances in planar lithographic techniques and the use of substrate steps to define microbridge dimensions have led to a number of successful approaches for making variable-thickness microbridges of dimension <0.1 μm. At this size scale, the step-edge approach is the simplest and most versatile technique for microbridge fabrication. The step-edge approach is also well suited to heated-substrate and multiple-material deposition. It thus provides an ideal vehicle for study of high-T_c refractory microbridges. Even for the smallest devices produced to date, however, the limits to device performance as dimensions are

[2] All devices of such small dimensions are of course sensitive to electrical burnout. Microbridges of the transition metals and alloys, with their higher melting temperatures, are expected to be less susceptible to burnout due to electrostatic discharge. It is our experience that with careful handling, like that required for MOSFET production, and with careful design of electrical measurements and shielding, virtually all burnout problems can be avoided. Significant care must be exercised, however.

reduced, or limits to scaling, have not yet been reached. There remains considerable room for ingenuity and for technical advance.

Acknowledgment

The research at Yale on edge-defined microbridges was done in collaboration with M. D. Feuer, to whom the author is indebted for many enlightening discussions and novel ideas.

References

[1] *Future Trends in Superconductive Electronics*, B. S. Deaver, C. M. Falco, J. H. Harris, and S. A. Wolf, Eds. New York: American Institute of Physics, 1978 (AIP Conf. Proc. 44).

[2] *IEEE Trans. Electron Devices*, vol. ED-27, Oct. 1980 (Special Issue on Josephson-Junction Devices).

[3] *IBM J. Res. Develop.*, vol. 24, no. 2, Mar. 1980 (Special Issue on Josephson Computer Technology).

[4] R. E. Howard, "Techniques for ultra-fine pattern generation," *Solid State Technol.*, vol. 23, pp. 127-132, Aug. 1980;
R. E. Howard and D. E. Prober, "Nanometer-scale fabrication techniques," in *VLSI Electronics-Microstructure Engineering*, vol. V, N. E. Einspruch, Ed. New York: Academic, 1981, to be published.

[5] M. R. Beasley, "Advanced superconducting materials for electronic applications," in [2, pp. 2009-2015];
M. R. Beasley and C. J. Kircher, "Josephson junction electronics: Materials issues and fabrication techniques," in *Proc. NATO Conf. on Superconducting Materials* (Sintra, Portugal, Aug. 1980), S. Foner and B. B. Schwartz, Eds. New York: Plenum, 1981, to be published.

[6] B. T. Ulrich and T. Van Duzer, "Fabrication of Josephson junctions," in *Superconductor Applications: SQUIDs and Machines*, Brian B. Schwartz and Simon Foner, Eds. New York: Plenum, 1977, pp. 321-354.

[7] L. D. Jackel, "Junction and circuit fabrication," in *SQUID '80*, H. D. Hahlbohm and H. Lübbig, Eds. New York: deGruyter, 1980, pp. 257-296.

[8] E. L. Hu, R. E. Howard, and L. D. Jackel, "High-resolution techniques for the fabrication of small-area Josephson tunnel junctions," this issue, pp. 1382-1385.

[9] J. E. Lukens, R. D. Sandell, and C. Varmazis, "Fabrication of microbridge Josephson junctions using electron beam lithography," in [1, pp. 298-311].

[10] K. K. Likharev, "Superconducting weak links," *Rev. Mod. Phys.*, vol. 51, pp. 101-159, Jan. 1979.

[11] W. J. Skocpol, "High frequency properties of microbridge and point contact Josephson junctions," in [1, pp. 335-339].

[12] M. Tinkham, "Junctions—types, properties, and limitations," in [1, pp. 269-279];
M. Tinkham, M. Octavio, and W. J. Skocpol, "Heating effects in high-frequency metallic Josephson devices: Voltage limit, bolometric mixing, and noise," *J. Appl. Phys.*, vol. 48, pp. 1311-1320, Mar. 1977.

[13] P. L. Richards and T-M. Shen, "Superconductive devices for millimeter wave detection, mixing, and amplification," in [2, pp. 1909-1920].

[14] J. Clarke, "Advances in SQUID magnetometers," in [2, pp. 1896-1908].

[15] G. Deutscher, "Granular superconductors for SQUIDs," in [1, pp. 397-403].

[16] J. H. Claassen, "Josephson behavior in granular NbN weak links," *Appl. Phys. Lett.*, vol. 36, pp. 771-773, May 1980. Ar-ion etching is currently employed in the fabrication procedure: J. H. Claassen, private communication.

[17] J. Warlaumont, J. C. Brown, and R. A. Buhrman, "Response times and low-voltage behavior of SNS microbridges," *Appl. Phys. Lett.*, vol. 34, pp. 415-418, Mar. 1979.

[18] M. D. Feuer and D. E. Prober, "Projection photolithography—Liftoff techniques for production of 0.2 μm metal patterns," this issue, pp. 1375-1378.

[19] R. B. Laibowitz, A. N. Broers, J.T.C. Yeh, and J. M. Viggiano, "Josephson effect in Nb nanobridges," *Appl. Phys. Lett.*, vol. 35, pp. 891-893, Dec. 1979;
R. F. Voss, R. B. Laibowitz, and A. N. Broers, "Niobium nanobridge dc SQUID," *Appl. Phys. Lett.*, vol. 37, pp. 656-658, Oct. 1, 1980.

[20] R. B. van Dover, R. E. Howard, and M. R. Beasley, "Fabrication and characterization of S-N-S planar microbridges," *IEEE Trans. Magnetics*, vol. MAG-15, pp. 574-577, Jan. 1979.

[21] M. D. Feuer and D. E. Prober, "Step-edge fabrication of ultrasmall Josephson microbridges," *Appl. Phys. Lett.*, vol. 36, pp. 226-228, Feb. 1980;
M. D. Feuer and D. E. Prober, "Static and dynamic properties of short, narrow, variable-thickness microbridges," *IEEE Trans. Magnetics*, vol. MAG-17, pp. 81-84, Jan. 1981.

[22] M. D. Feuer, Ph.D. thesis, Yale Univ., 1980 (available from University Microfilms, Ann Arbor, MI).

[23] R. Laibowitz, A. Broers, D. Stroud, and B. R. Patton, "Ratio of superconducting transition temperatures in granular Nb films," *Amer. Inst. Phys. Conf. Proc.*, vol. 58, pp. 278-281, 1980.

[24] T. W. Lee and C. M. Falco, "Josephson effects in ultrashort mean-free-path superconductors," *Appl. Phys. Lett.*, vol. 38, pp. 567-569, Apr. 1, 1981; J. E. Mercereau and H. A. Notarys, "Thin film superconducting devices," *J. Vac. Sci. Technol.*, vol. 10, pp. 646-651, Sept./Oct., 1973.

[25] A. de Lozanne, M. Dilorio, and M. R. Beasley "Properties of high-T_c SNS microbridges," in *Proc. Sixteenth Int. Conf. on Low Temp. Phys.*, Los Angeles, CA, Aug. 1981, *Physica*, vol. 108B, pp 1027-1028, 1981.

[26] H. Ohta, "A new Josephson junction with a very short barrier length and a very low capacitance," in [2, pp. 2027-2029].

[27] H. W. Lehmann and R. Widmer, "Profile control by reactive sputter etching," *J. Vac. Sci. Technol.*, vol. 15, pp. 319-326, Mar./Apr. 1978.

[28] R. C. Ruby and T. Van Duzer, "Silicon-coupled Josephson junctions and super-Schottky diodes with coplanar electrodes," this issue, pp. 1394-1397.

[29] D. A. Weitz, W. J. Skocpol, and M. Tinkham, "Characterization of niobium point contacts showing Josephson effects in the far infrared," *J. Appl. Phys.*, vol. 49, pp. 4873-4880, Sept. 1978.